# Anharmonic order-parameter oscillations and lattice coupling in strongly driven charge-density-wave compounds: A multiple-pulse femtosecond laser spectroscopy study

P. Kusar[1], T. Mertelj[1], V.V. Kabanov[1], J.-H. Chu[2], I. R. Fisher[2], H. Berger[3], L. Forró[3], D. Mihailovic[1]
[1] *Complex Matter Dept., Jozef Stefan Institute, Jamova 39, Ljubljana, SI-1000, Ljubljana, Slovenia*
[2] *Geballe Laboratory for Advanced Materials, Dept. of Applied Physics, Stanford University, California 94305, USA and*
[3] *Physics Department, EPFL CH-1015 Lausanne, Switzerland*
(Dated: October 11, 2010)

The anharmonic response of charge-density wave (CDW) order to strong laser-pulse perturbations in $1T$-$TaS_2$ and $TbTe_3$ is investigated by means of a multiple-pump-pulse time-resolved femtosecond optical spectroscopy. We observe remarkable anharmonic effects hitherto undetected in the systems exhibiting collective charge ordering. The efficiency for additional excitation of the amplitude mode by a laser pulse becomes periodically modulated after the mode is strongly excited into a coherently oscillating state. A similar effect is observed also for some other phonons, where the cross-modulation at the amplitude-mode frequency indicates anharmonic interaction of those phonons with the amplitude mode. By analyzing the observed phenomena in the framework of time-dependent Ginzburg-Landau theory we attribute the effects to the anharmonicity of the mode potentials inherent to the broken symmetry state of the CDW systems.



Ultrashort laser pulses are a convenient tool for coherent excitation of phonons[1, 2] and collective electronic-lattice modes in CDW systems[3–6]. Due to availability of strong laser pulses the phonons can be driven far from equilibrium exposing anharmonic effects. The high excitation region has been already investigated with single-pump-pulse[7–9] and double-pump-pulse[10–12] sequences, mainly in elemental Bi, Sn and Te.

In charge density wave (CDW) systems the phonon mode potentials are inherently anharmonic due to their coupling to the electron density modulation.[13] The anharmonicity is the strongest for the Kohn-anomaly[14] modes which become the amplitude and phase modes in the CDW state. While amplitude modes (AM) have been extensively investigated in the near equilibrium conditions by Raman[14, 15] and time resolved spectroscopy[3–6, 16] and in the highly driven non-equilibrium conditions, where the CDW order is destroyed[17–20], so far little attention[18] has been paid in the region inbetween.

Here we report on an investigation of a new hitherto unexplored aspect of the CDW amplitude mode behavior under strongly driven non-equilibrium conditions in the ordered phase below the CDW photoinduced destruction threshold. Contrary to previous standard double-pump pulse (SDPP) high-excitation works[10–12], where a pair of balanced[32] pump pulses was used, we introduce a novel *unbalanced double-pump-pulse* (UDPP) approach in which we use the first and the strongest pump pulse ($P_1$) to excite large-amplitude coherent oscillations of the AM and other phonon modes and then use a standard pump-probe ($P_2$-$p_3$) pulse sequence to interrogate the system. By means of this novel approach we are able to directly investigate the anharmonicity of the effective AM potential, as well as detect the anharmonic coupling of the collective bosonic mode (the AM) of the CDW to other lattice modes.

To establish generality, two layered chalcogenides which show different types of CDW ordering and also different electronic properties, were investigated: $TbTe_3$ and $1T$-$TaS_2$.[33] $TbTe_3$ is a two-dimensional (2D) metal which shows an unidirectional incommensurate CDW state at the temperature used in our experiment (15 K),[21, 22] while $1T$-$TaS_2$ is in a commensurate insulating CDW state at the relevant temperature (77K)[23]. In both systems, in addition to the AM, several new Raman modes appear in the CDW state due to Brillouin-zone folding.[4, 6, 14, 24, 25]

In our experiments the three pulse trains were derived from a 50-fs 250-kHz Ti:$Al_2O_3$ regenerative amplifier, with $\hbar\omega_P = 1.55$ eV photon energy. The $p_3$ polarization was perpendicular to $P_1$ and $P_2$, which were parallel. To study the reflectivity change induced by the weaker $P_2$ pulse, $\Delta R_2(t)$, we eliminate the $P_1$ contribution, $\Delta R_1(t)$, to the total transient reflectivity, $\Delta R(t)$, by means of the homodyne detection locked to the modulation of the $P_2$ pulse train. [The $P_1$ pulse train was unmodulated as shown in Fig 1(b).]

In Fig. 1(a) we plot the raw UDPP photoinduced reflectivity transients, $\Delta R_2(t_{23})/R$, in $1T$-$TaS_2$ at different delays, $t_{12}$, between the pump pulses. The intensity of the $P_2$ pulse train, $I_2$, was set in the linear response region while the intensity of the $P_1$ pulse train was 4-times larger corresponding to ∼30% of the CDW destruction treshold fluence. For comparison the raw total photoinduced reflectivity transients $\Delta R(t_{23})/R$, measured in SDPP configuration, are shown in Fig. 1(c). In both cases the amplitude of the coherent oscillations periodically varies as $t_{12}$ is increased with a clear periodic suppression of the oscillations. Note that the suppression appears at *different* $t_{12}$ for each case. While

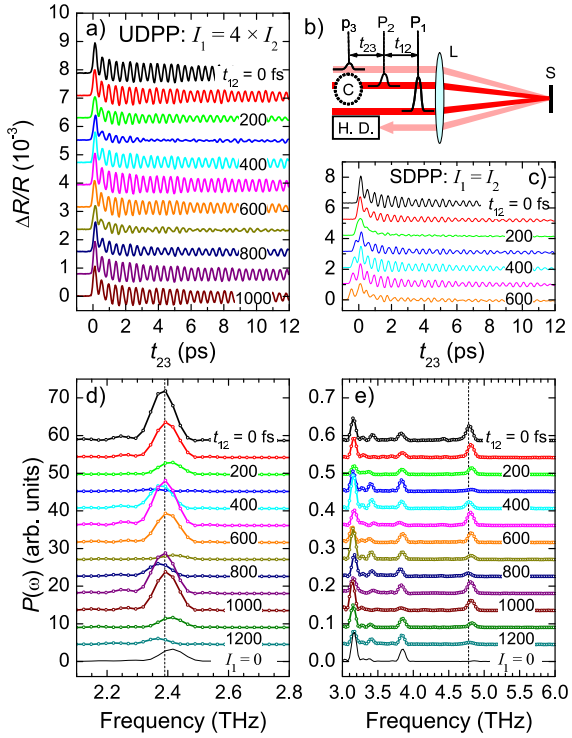


Figure 1: (Color online) $\Delta R/R$ transients as a function of $t_{12}$ in 1$T$-$TaS_2$ in the UDPP configuration (a) as shown in the schematics (b), L - lens, S - sample, C - chopper, H.D. - homodyne detection system. For comparison $\Delta R/R$ transients in the SDPP configuration are shown in (c). UDPP power spectra in 1$T$-$TaS_2$ around the fundamental frequency of the strongest mode (d) and around the second harmonic of the fundamental frequency (e). The thin curve in (d) and (e) is the standard single pump-pulse spectrum.

the linear SDPP effect [Fig. 1(c)] is well known[16, 26–28], and is understood as an interference due to the linear superposition of two independently excited coherent oscillations[16, 27, 28], the nonlinear effects observed by UDPP are completely new and hitherto undetected.

In Fig. 1(d), (e) we plot the power spectra of the UDPP transients from Fig. 1(a). In addition to the AM mode with the frequency 2.41 THz we observe several weaker phonon modes above 3 THz and a weak second harmonic of the AM mode [see 1(e)]. The periodic intensity modulation of the modes, which strongly increases with increasing $I_2$ (see Fig. 2), is accompanied with a small periodic frequency shift. The shift is absent in the low-excitation SDPP configuration [see Fig. 2(c) and (f)]. The modulation amplitude and phase vary among the modes and there is a $\sim \pi/2$ shift between the modulation phases of the UDPP and SDPP case, similar to the observations in the high-excitation-density SDPP experiment in Te.[11] In our case however, the phase shift persists down to the lowest excitation density.

The periodic intensity modulation and the phase shift are observed also in $TbTe_3$, where in addition a beating in the $t_{12}$ dependence of the modulation amplitudes is observed (see Fig. 3(c)).

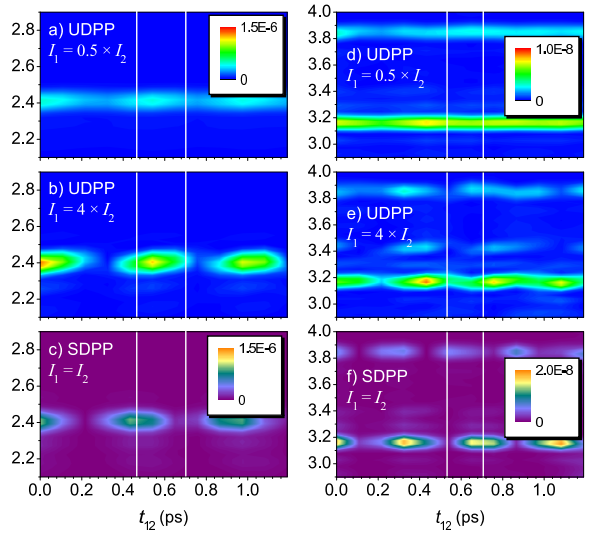


Figure 2: (Color online) Spectra of the strongest mode (a), (b) and weaker modes (d), (e) as functions of $t_{12}$ in the UDPP configuration at different intensities of the $P_1$ pulse train in 1$T$-$TaS_2$. For comparison the low-excitation SDPP-configuration spectra are shown in (c) and (f).

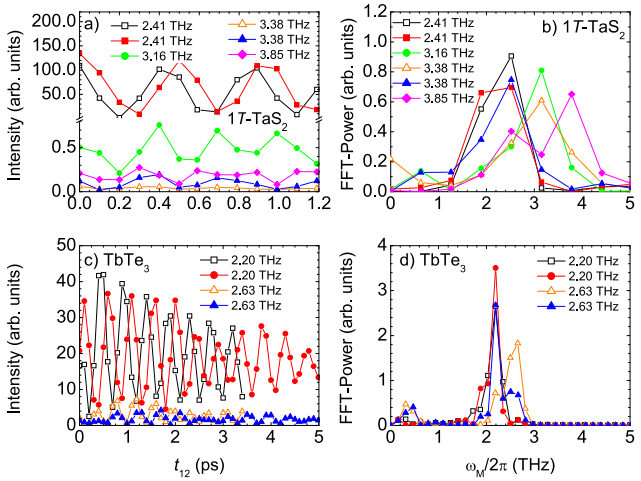


Figure 3: (Color online) Integrated intensities of the strongest modes as functions of $t_{12}$ in UDPP configuration at $I_1 = 4 \times I_2$ in 1$T$-$TaS_2$ (a) and at $I_1 = 2.4 \times I_2$ in $TbTe_3$ (c). Normalized power spectra of the traces in the left panels (b) and (d). Open symbols correspond to the low-intensity SDPP response. Note the difference in the modulation frequency for the 3.38-THz mode in 1$T$-$TaS_2$ (b) and 2.63-THz mode in $TbTe_3$ (d) between the UDPP (full triangles) and SDPP (open triangles) cases.

The modulation frequency of each mode [see Fig. 3

(b) and (d)] is correlated to the respective mode eigenfrequency. Surprisingly, in the UDPP configuration there is also a clear *cross-modulation* of the 3.38-THz and 3.85-THz mode intensities with the 2.41-THz AM frequency and the 2.63-THz mode intensity with the 2.20-THz AM frequency in $1T$-$TaS_2$ and $TbTe_3$, respectively.

To understand the observed phenomena we start with the simplest Ginzburg-Landau expansion of the free energy:

$$F = F_0 + \left(\frac{T}{T_c} - 1\right)|A|^2 + \frac{1}{2}|A|^4 + g(t)|A|^2, \quad (1)$$

in terms of the normalized complex order parameter, $A$. $T_c$ is the critical temperature and $g(t)$ represents the external laser excitation. Due to the symmetry $g(t)$ can only couple to $|A|^2$. To describe the dynamics we introduce the $T = 0$ AM frequency, $\omega_0$, and the dimensionless damping, $\gamma = \Delta\omega_0/\omega_0$, and obtain using (1):

$$\frac{2}{\omega_0^2}\frac{\partial^2}{\partial t^2}A + \frac{4\gamma}{\omega_0}\frac{\partial}{\partial t}A + \left(\frac{T}{T_c} - 1\right)A + |A|^2 A = -g(t)A. \quad (2)$$

Since $g(t)A$ can not excite phase fluctuations[34], only the AM needs to be considered. The dielectric constant depends in the lowest order on $|A|^2$:[29]

$$\epsilon = \epsilon_0 + c_1|A|^2, \quad (3)$$

so the reflectivity change in the UDPP configuration is written as:

$$\Delta R_2(t) = \Delta R(t) - \Delta R_1(t) \propto |A(t)|^2 - |A_1(t)|^2, \quad (4)$$

where $A_1(t)$ is the solution of equation (2) with excitation from the $P_1$ pulse only and $A(t)$ the solution with the excitation from both pump pulses.

There are two terms in (2) that are of interest: $g(t)A$ and $|A|^2A$. The term $g(t)A$ leads to a periodic modulation of the coupling of $A$ to the $P_2$ pulse when the oscillation amplitude after the $P_1$ pulse is large. This effect however does not explain the main features of our observations: (i) if the oscillation amplitude is large, a significant AM-overtone intensity is expected due to $|A|^2$ in (3), which is not observed in the experiment, (ii) because the laser excitation initially drives $A$ towards zero[35] an intermediate amplitude of the oscillations at $t_{12} = 0$ followed by a minimum at $\omega_0 t_{12} \simeq \pi/2$, where $A(t)$ is closest to 0, is expected. Instead, the first minimum is observed around $\omega_0 t_{12} \simeq 3\pi/2$ and the amplitude is the largest at $t_{12} = 0$ in $1T$-$TaS_2$ and at $\omega_0 t_{12} \simeq \pi/2$ in $TbTe_3$. The anharmonic term $|A|^2A$ in (2) remains therefore the only possible origin of the observed behavior.

The solutions of equation (2) with $\gamma = 0$ can be represented as closed periodic orbits in the phase space (see Fig. 4 (a)). Due to the anharmonicity the frequency of the orbit decreases with the oscillation amplitude. The $P_2$ pulse transfers the system from the initial orbit, set by the $P_1$ pulse, to a final orbit with a different frequency which depends on $t_{12}$. This results in a beating of the $\Delta R_2(t)$ oscillations due to an interference of the second and the first term in the right hand side of (4) corresponding to the initial and final orbits, respectively. The frequency of the final orbit periodically oscillates with increasing $t_{12}$ [see Fig. 4 (b)]. Within a single initial orbit period there exist two delays, $\omega_0 t_{12} \sim \phi_0 + \pi/2$ and $\sim \phi_0 + 3\pi/2$, at which the only effect of the $P_2$ pulse is a phase shift within the initial orbit. In vicinity of these delays the beating is very slow resulting in a slow increase of the $\Delta R_2(t)$ oscillations amplitude with $t$. This slow rise is suppressed when $\gamma$ is finite since the oscillations die out before a significant phase shift between the orbits builds up and the $\Delta R_2(t)$ oscillations amplitude remains small. As a result a periodic modulation of the $\Delta R_2(t)$ oscillations amplitude is observed in the simulations with finite $\gamma$ [see Fig. 4 (c)]. In addition to the more intensive maximum, reminiscent to the experimental observations, an additional weak maximum is observed within a single period corresponding to $t_{12}$ with the the larger final-orbit frequency [see Fig. 4 (b)]. The weak maximum is strongly sensitive to the characteristic timescale of the external laser perturbation, $\tau_g$,[36] and is completely suppressed by setting $\tau_g = 2\pi/\omega_0$ as shown in Fig. 4 (d).

To improve agreement of the model with the experiment we extended the Ginzburg-Landau expansion (1) with the gradient term, $\xi^2|\partial A/\partial z|^2$,[20] to allow for space variations of the order parameter perpendicular to the sample surface due to the finite penetration depth, $\lambda$, of the laser pulses. The result of a simulation with the inhomogeneous order parameter [Fig. 4 (e)] better reproduces the main experimental features for the AM. Similarly to the homogeneous case the weak maximum, which is not observed in the experiment, is absent only for long enough $\omega_0\tau_g \sim 2\pi$. In our experiment $\omega_0\tau_l \sim 0.2\pi$, where $\tau_l$ is the length of the laser pulses, indicating that the coherent oscillations are not excited by the impulsive stimulated-Raman-scattering mechanism[2], but rather by the displacive one[1], which can lead to $\tau_g > \tau_l$.

Counter intuitively, the experimentally observed small periodic frequency modulation of the AM is not reproduced in any simulation with a finite damping so the origin of the effect is beyond the present model.

Next we turn to analysis of the weaker modes with displacements denoted $Q_i$. Similarly to the AM we can exclude the direct driving terms, $|Q_i|^2 g(t)$ and $\Re(Q_i A^*)g(t)$, as the sources of the modulation due to the relatively small displacements. However, in addition to the AM also other modes are coupled to the CDW charge modulation. As a result, mode displacements $Q_i$ become mixed with the AM displacement[37] $A$ and the effective mixed-mode potentials become anharmonic. This leads to the *cross-modulation* of mode intensities with the AM

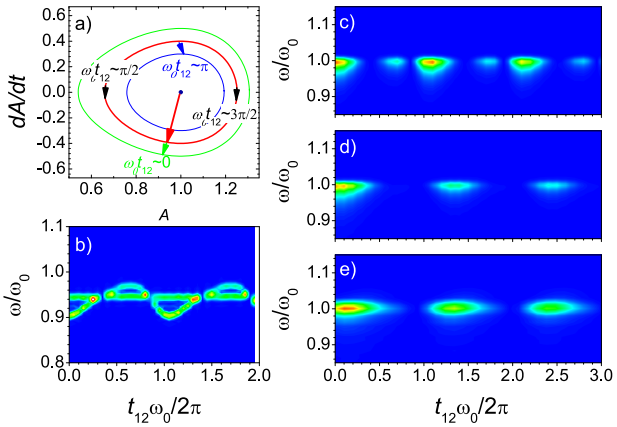


Figure 4: (Color online) Orbits of eq. (2) in the phase space in the absence of damping ($\gamma = 0$) (a). The long arrow represents the initial excitation by the $P_1$ pulse. The short arrows represent the additional excitation by the $P_2$ pulse which transfers the system to different orbits depending on $t_{12}$. Simulated power spectrum as a function of $t_{12}$ in the absence of damping (b), with damping ($\gamma = 0.01$) and short excitation pulses, $\omega_0\tau_g = 0.2\pi$ (c), with damping and long excitation pulses $\omega_0\tau_g = 2\pi$ (d), with damping, long excitation pulses and finite laser penetration depth, $\lambda/\xi$=16, (e).

frequency in addition to the self-modulation at the particular mode eigenfrequency. The relative amounts of the modulation at both frequencies depend on the couplings to the AM and to the external laser perturbation. If after the $P_1$ pulse the amplitude of a particular mode is small the main contribution to the modulation is due to the cross-modulation at the AM frequency, as is the case for the 3.38-THz mode in 1$T$-$TaS_2$ and the 2.63-THz mode in $TbTe_3$. If, on the other hand, the amplitude is large enough a significant self-modulation is expected as in the case of the 3.85-THz in 1$T$-$TaS_2$.

In conclusion, by means of a novel *unbalanced double-pump-pulse* time resolved optical spectroscopy, we were able to detect the inherent broken-symmetry-state anharmonicity of the amplitude-mode effective potential in two distinct CDW systems. We also found a clear evidence of the anharmonic mixing of certain phonon modes with the amplitude mode originating from their mutual coupling to the electronic-density CDW modulation. We showed that the observed effects can be described in the framework of time dependent Ginzburg-Landau theory.

This work has been supported by Slovenian Research Agency and the CENN Nanocenter.

[1] H. J. Zeiger, J. Vidal, T. K. Cheng, E. P. Ippen, G. Dresselhaus, and M. S. Dresselhaus, Phys. Rev. B **45**, 768 (1992).
[2] R. Merlin, Solid State Communications **102**, 207 (1997).
[3] J. Demsar, K. Biljakovic, and D. Mihailovic, Phys. Rev. Lett. **83**, 800 (1999).
[4] J. Demsar, L. Forró, H. Berger, and D. Mihailovic, Phys. Rev. B **66**, 041101 (2002).
[5] D. Sagar, A. Tsvetkov, D. Fausti, S. van Smaalen, and P. van Loosdrecht, Journal of Physics: Condensed Matter **19**, 346208 (2007).
[6] R. V. Yusupov, T. Mertelj, J.-H. Chu, I. R. Fisher, and D. Mihailovic, Phys. Rev. Lett. **101**, 246402 (2008).
[7] S. Hunsche, K. Wienecke, T. Dekorsy, and H. Kurz, Phys. Rev. Lett. **75**, 1815 (1995).
[8] M. Hase, M. Kitajima, S.-i. Nakashima, and K. Mizoguchi, Phys. Rev. Lett. **88**, 067401 (2002).
[9] O. V. Misochko, M. Hase, K. Ishioka, and M. Kitajima, Phys. Rev. Lett. **92**, 197401 (2004).
[10] M. F. DeCamp, D. A. Reis, P. H. Bucksbaum, and R. Merlin, Phys. Rev. B **64**, 092301 (2001).
[11] C. A. D. Roeser, M. Kandyla, A. Mendioroz, and E. Mazur, Phys. Rev. B **70**, 212302 (2004).
[12] E. D. Murray, D. M. Fritz, J. K. Wahlstrand, S. Fahy, and D. A. Reis, Phys. Rev. B **72**, 060301 (2005).
[13] H. Schäfer, V. V. Kabanov, M. Beyer, K. Biljakovic, and J. Demsar, Phys. Rev. Lett. **105**, 066402 (2010).
[14] S. Sugai, Phys. Status Solidi B **129**, 13 (1985).
[15] M. Lavagnini, M. Baldini, A. Sacchetti, D. Di Castro, B. Delley, R. Monnier, J.-H. Chu, N. Ru, I. R. Fisher, P. Postorino, et al., Phys. Rev. B **78**, 201101 (2008).
[16] T. Onozaki, Y. Toda, S. Tanda, and R. Morita, Japanese Journal of Applied Physics **46**, 870 (2007).
[17] L. Perfetti, P. A. Loukakos, M. Lisowski, U. Bovensiepen, H. Berger, S. Biermann, P. S. Cornaglia, A. Georges, and M. Wolf, Phys. Rev. Lett. **97**, 067402 (2006).
[18] F. Schmitt, P. Kirchmann, U. Bovensiepen, R. Moore, L. Rettig, M. Krenz, J. Chu, N. Ru, L. Perfetti, D. Lu, et al., Science **321**, 1649 (2008).
[19] A. Tomeljak, H. Schäfer, D. Städter, M. Beyer, K. Biljakovic, and J. Demsar, Phys. Rev. Lett. **102**, 066404 (2009).
[20] R. V. Yusupov, T. Mertelj, P. Kusar, V. Kabanov, S. Brazovskii, J.-H. Chu, I. R. Fisher, and D. Mihailovic, Nature Physics **6**, 681 (2010).
[21] E. DiMasi, M. C. Aronson, J. F. Mansfield, B. Foran, and S. Lee, Phys. Rev. B **52**, 14516 (1995).
[22] A. Fang, N. Ru, I. R. Fisher, and A. Kapitulnik, Phys. Rev. Lett. **99**, 046401 (2007).
[23] R. E. Thomson, B. Burk, A. Zettl, and J. Clarke, Phys. Rev. B **49**, 16899 (1994).
[24] T. Hirata and F. S. Ohuchi, Solid State Communications **117**, 361 (2001), ISSN 0038-1098.
[25] M. Lavagnini, H. Eiter, L. Tassini, B. Muschler, R. Hackl, R. Monnier, J. Chu, I. Fisher, and L. Degiorgi, Arxiv preprint arXiv:0909.1289 (2009).
[26] T. Dekorsky, W. Kütt, T. Pfeifer, and H. Kurz, EPL (Europhysics Letters) **23**, 223 (1993).
[27] M. Hase, K. Mizoguchi, H. Harima, S. Nakashima, M. Tani, K. Sakai, and M. Hangyo, Applied Physics Letters **69**, 2474 (1996).
[28] D. Mihailovic, D. Dvorsek, V. Kabanov, J. Demsar, L. Forro, and H. Berger, Appl Phys Lett **80**, 871 (2002).
[29] V. Ginzburg, A. Levanyuk, and A. Sobyanin, Physics Reports **57**, 151 (1980).
[30] N. Ru, J.-H. Chu, and I. R. Fisher, Phys. Rev. B **78**, 012410 (2008).
[31] B. Dardel, M. Grioni, D. Malterre, P. Weibel, Y. Baer, and F. Lévy, Phys. Rev. B **45**, 1462 (1992).

[32] The fluences of the pulses were chosen such to achieve a complete suppression of the coherent oscillation at certain interpulse delays.
[33] Sample growth is described in ref. [30] for $TbTe_3$ and ref. [31] for $1T$-$TaS_2$.
[34] In the equilibrium, $A$ can be always be set real by a proper choice of the phase.
[35] $g(t)$ couples to $A$ as $T$ so a positive $g(t)$ decreases $A$.
[36] In simulations $g(t) = g_1 f(t) + g_2 f(t - t_{12})$ with $f(t) = \exp(-t/\tau_g)/[1 + \exp(-10t/\tau_g)]$ was used to represent $P_1$ and $P_2$.
[37] The terms $\Re(Q_i A^*)$ must be added to the total free energy.